

Molecular-dynamics simulations of polyampholytes: Instabilities due to excess charges and external fields

T. Soddemann,* H. Schiessel,† and A. Blumen

Institut für Theoretische Polymerphysik, Universität Freiburg, Rheinstrasse 12, D-79104 Freiburg, Germany

(Received 6 August 1997)

In this paper we study the conformational properties of polyampholytes (PAs; polymers with positively and negatively charged monomers) by molecular-dynamics (MD) simulations and by scaling arguments. As is well known, in the absence of external electrical fields PAs with a small total charge Q_{tot} collapse into spherical globules, whereas PAs whose Q_{tot} exceeds a critical value Q_c are expanded; our MD simulations confirm this fact. For $Q_{\text{tot}}=0$ we study the influence of external electric fields on single PAs. We find that the PA globule is unstable above a critical field strength E_{c1} ; for $E>E_{c1}$ the PA becomes highly stretched. Lowering the external field again, one observes hysteresis; the PA collapses back into a globule only for $E<E_{c2}$ where $E_{c2}<E_{c1}$. In the weak coupling limit (when the intrachain electrostatic interactions can be neglected) the PA attains in an external field a trumpetlike shape, whose end-to-end distance obeys Pincus scaling. [S1063-651X(98)15102-4]

PACS number(s): 36.20.Ey, 64.60.My, 87.15.By

I. INTRODUCTION

Polyampholytes (PAs) are heteropolymers carrying quenched positive and negative charges along their backbone; the investigation of their conformational and dynamical properties is of much current interest [1–35]. A characteristic feature of PAs is the competing interactions among the charged monomers. PAs are thus reminiscent of proteins, whose amino acid sequences induce their specific unique conformations [36–39]. From a more general point of view PAs may be seen as being soft-matter counterparts to random systems with competing interactions such as spin glasses [40,41].

Neutral PA chains (for which the total charge Q_{tot} is zero) usually collapse into spherical globules; the mechanism underlying this phenomenon is the tendency of the charges to screen each other in Debye-Hückel-like fashion [4,9,28]. In the general case there exist several mechanisms which work against this collapse; we mention here two of them. (a) The PA may carry an excess charge $Q_{\text{tot}}\neq 0$ which cannot be screened and which tends to expand the chain [12,14–17]. (b) In the presence of an external field E , different portions of the chains are pulled in different directions [26,28,32].

An interesting question is whether there is a critical overall charge Q_c (or a critical field strength E_c) which separates the collapsed from the stretched states. In case (a) scaling arguments as well as numerical simulations show that the globular state becomes indeed unstable above a critical excess charge $Q_c\approx\pm q\sqrt{N}$ [16]; this is supported by experimental works, which indicate that PAs exist both in globular and in stretched forms [7,11]. On the other hand, in case (b) the crossover from a globular to a stretched state was in-

ferred only based on different scaling arguments (namely, on the droplet picture in Refs. [26,28] and on a coexistence argument in Ref. [32]).

The purpose of this paper is to investigate both cases (a) and (b) by means of molecular-dynamics (MD) simulations, and to compare the results with the theoretical predictions; we devote Secs. II and IV of this article to this effect. In Sec. III we study the behavior of PAs in external fields in the weak coupling limit (WCL). In the WCL the mutual interaction between the intrachain charges can be neglected; this situation is realized by relatively short PAs, in which only a small fraction of the monomers carries charges. We remark that in the WCL many properties of PAs in Θ solvents can be calculated exactly [18,20,24,28,29]; on the other hand, in good solvents (where excluded volume effects come into play) one has to resort to scaling arguments [26,28]. In this paper we succeed in supporting several of these results by MD simulations. We close the paper in Sec. V with a summary of conclusions.

II. POLYAMPHOLYTES: THE ROLE OF THE EXCESS CHARGE

In this section we study the behavior of single PA chains in the absence of counterions and external electrical fields. Then three effects determine the conformation of the PAs. (i) On entropic grounds the PAs favor Gaussian shapes in Θ solvents or swollen conformations in good solvents; the volume obeys then $V\cong b^3N^{3\nu}$, where b denotes the average bond length, N is the number of monomers of the PA, and the exponent ν equals $\frac{1}{2}$ for Gaussian chains and $\frac{3}{5}$ for swollen chains. (ii) Fluctuations in the local charge distribution favor the collapse of the PAs; (iii) large, noncompensated excess charges Q_{tot} tend to extend the PAs.

We consider first a PA with vanishing total charge, $Q_{\text{tot}}=0$, so that only effects (i) and (ii) come into play. Let fN monomers (with $f\leq 1$) carry charges, $(f/2)N$ of which are positively ($+q$) and $(f/2)N$ negatively ($-q$) charged. We assume that the charges are randomly distributed over the PA

*Present address: Max-Planck-Institut für Polymerforschung, Ackermannweg 10, 55128 Mainz, Germany.

†Present address: Materials Research Laboratory, University of California at Santa Barbara, Santa Barbara, CA 93106-5130.

and form a quenched pattern. It is known [4,9] that such PAs collapse in general into spherical globules, whose volume V is significantly smaller than that of the uncharged species $b^3N^{3\nu}$, but much larger than that of the most dense monomer packing b^3N , i.e., one has $b^3N \ll V \ll b^3N^{3\nu}$. Higgs and Joanny [4] estimated the volume of PAs in this regime in analogy to electrolytes (based on Ref. [1] by Edwards, King, and Pincus). Reference [4] starts from the Debye-Hückel approximation and leads to the following simple picture [4,28]: The conformation of the PA may be seen as being a densely packed assembly of blobs, whose linear size is the Debye-screening length $r_D = \sqrt{V/(fNl_B)}$; here $l_B = q^2/(\epsilon T)$ is the Bjerrum length, ϵ denotes the dielectric constant, and T is the thermal energy expressed in units of the Boltzmann constant k_B . Each of these Debye blobs has an electrostatic energy (self-energy as well as interaction energy with neighboring blobs) of the order of T ; thus each blob follows the statistics of an ideal or of a real chain closely, i.e., the size of the blob, r_D , and the number of its monomers, g , are related by $r_D \cong bg^\nu$. The overall electrostatic energy F_e of the PA follows simply from $F_e = -(V/r_D^3)T$, which leads to the classical result of the Debye-Hückel approximation [42]

$$\frac{F_e}{T} = -\frac{(fNl_B)^{3/2}}{V^{1/2}} = -\frac{fNl_B}{r_D}. \quad (1)$$

Furthermore the volume of the globule is given by the volume of its N/g Debye blobs, i.e., by $V \cong (N/g)r_D^3$, from which it follows that

$$V \cong b^3N \left(\frac{b}{fl_B} \right)^{(3\nu-1)/(1-\nu)} = \begin{cases} b^3N \frac{b}{fl_B} & \text{for } \nu = \frac{1}{2} \\ b^3N \left(\frac{b}{fl_B} \right)^2 & \text{for } \nu = \frac{3}{5}. \end{cases} \quad (2)$$

The Flory-type argument presented in Ref. [4] (cf. also Refs. [9,28]) leads to the same results, Eqs. (1) and (2).

Note that these approaches are only valid as long as $b \ll r_D \ll bN^\nu$ (or equivalently $b^3N \ll V \ll b^3N^{3\nu}$). For $b \approx r_D$ the electrostatic interaction between neighboring charges is of the order of the thermal energy, so that the conformation is practically frozen in; on the other hand, for $r_D \approx bN^\nu$ the whole PA is a simple Debye blob and the shape of the chain is unaffected by the interaction between the charges. The Debye-Hückel condition $b^3N \ll V \ll b^3N^{3\nu}$ can be reformulated [28] as

$$fl_B \ll b \ll fN^{1-\nu}l_B. \quad (3)$$

On the other hand, when one has

$$b > fN^{1-\nu}l_B \quad (4)$$

the electrostatic interaction between the charges is smaller than the thermal effects, a situation called the weak-coupling limit; in this case the PA takes the usual Gaussian (Θ solvent) or self-avoiding walk (good solvent) forms. As an example one has $l_B \cong 7 \text{ \AA}$ for water at room temperature; thus condition (4) is readily fulfilled for not-too-long PA chains with a sufficiently low density f of charges.

Now, let us study PAs with a nonvanishing total charge and discuss the role of effect (iii). We follow here an argument by Kantor and Kardar [16], who estimated the typical electrostatic energy of PAs at high temperatures. Consider again PA chains with fN charged monomers, but now having a nonvanishing Q_{tot} . Thus out of the fN charged monomers, N_+ monomers carry the charge $+q$ and N_- monomers carry the charge $-q$, so that $N_+ + N_- = fN$ and $N_+ - N_- = Q_{\text{tot}}/q$ hold. We denote by q_n the charge of the n th monomer ($n = 1, \dots, N$); hence $Q_{\text{tot}} = \sum_n q_n$. Let us consider now all the different possible realizations of the $\{q_n\}$ sequences. Denoting by angular brackets the average over all these distributions one has [16]

$$\langle q_i q_j \rangle = \begin{cases} fq^2 & \text{for } i=j \\ \frac{Q_{\text{tot}}^2 - q^2 fN}{N(N-1)} & \text{for } i \neq j. \end{cases} \quad (5)$$

At sufficiently high temperatures the shape of the PA is quite undisturbed by the charges, and its radius of gyration R_g obeys $R_g \propto N^\nu$. Using Eq. (5) and taking R_g as a measure of the typical interparticle distance one finds for the electrostatic energy

$$\overline{\langle U_e \rangle} \cong \epsilon^{-1} \sum_{i \neq j} \langle q_i q_j \rangle / r_{ij} \cong \frac{Q_{\text{tot}}^2 - q^2 fN}{\epsilon R_g}, \quad (6)$$

where the overbar denotes thermal averaging and $r_{ij} = |\mathbf{r}_i - \mathbf{r}_j|$ is the distance between monomers i and j . Note that $Q_c = q\sqrt{fN}$ is a critical value for Q_{tot} , since at Q_c the function $\overline{\langle U_e \rangle}$ changes its sign. Let us now set $T_{Q_{\text{tot}}} = |\overline{\langle U_e \rangle}|$. For $T \gg T_{Q_{\text{tot}}}$ the electrostatic energy can be ignored. If $T \approx T_{Q_{\text{tot}}}$ the electrostatic energy influences the shape of the PA: With decreasing temperature PAs with $Q_{\text{tot}} < Q_c$ will lower $\overline{\langle U_e \rangle}$ by shrinking, whereas PAs with $Q_{\text{tot}} > Q_c$ will expand. Note that for $Q_{\text{tot}} = 0$ the condition for the WCL, $b > fN^{1-\nu}l_B$ [cf. Eq. (4)] is equivalent to $T_{Q_{\text{tot}}=0} > |\overline{\langle U_e \rangle}|$.

These qualitatively determined features are also supported numerically, as shown by Kantor and Kardar [16], who performed Monte Carlo simulations using the bond-fluctuation method [43,44]. Here we reproduce and extend some of their results using, however, a molecular-dynamics approach (for a detailed discussion of MD see Ref. [45]). MD simulations are especially suitable in order to investigate the response of PAs to external electrical fields (we will show this in Secs. III and IV). We let the potential U_{ij} between beads i and j consist of three parts, i.e., $U_{ij} = U_{ij}^0 + U_{ij}^{ch} + U_{ij}^C$, as follows: (a) The shifted, purely repulsive Lennard-Jones potential U_{ij}^0 accounts for the excluded volume of the monomers [45]; (b) U_{ij}^{ch} takes into account the connectivity between nearest neighbors [45]; (c) U_{ij}^C represents the Coulombic interaction between charged monomers and is given by $U_{ij}^C(r) = q_i q_j / r_{ij}$ (here we set $\epsilon = 1$).

We now display the results of MD simulations, using PAs consisting of 64 monomers, i.e., $N = 64$. We start with a situation in which each monomer is charged, thus $f = 1$. The other parameters are taken to be (here and in the following) $q = 1$ and $b \cong 1$. Figure 1 displays R_g^2 as a function of temperature; each curve depends parametrically on the fixed excess charge Q_{tot} (the different curves are marked by Q_{tot}/q).

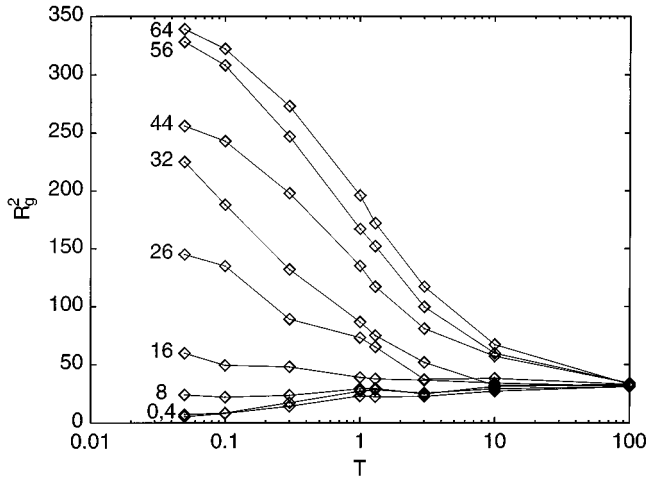


FIG. 1. R_g^2 ($b=1$) as a function of T for different values of the excess charge Q_{tot} for a 64-monomer chain. Each point is an average over ten independent runs at each temperature. The numbers near each curve denote Q_{tot} (in units of q).

For any given Q_{tot} there are many different realizations of charge distributions; in Fig. 1 each data point is an average over ten different, randomly chosen quenched realizations. The smoothness of the different curves shows that R_g^2 is mainly determined by Q_{tot} , whereas the dependence on the chosen set of quenched distributions is quite small (see also the more detailed analysis of the quenched averaging procedure by Kantor and Kardar [16]). We observe that at high temperatures, $T \approx 100$, the electrostatic interaction between the monomers is unimportant (WCL case): All configurations behave as self-avoiding random walks with $R_{g,0} \propto N^\nu$, where $\nu \approx \frac{3}{5}$. With decreasing temperature the interactions between the charges begin to become relevant and induce changes in the shape of the PAs. At $T \approx 10$ the R_g of the highly charged PAs (with $Q_{\text{tot}}=44, 56$, and 64) shows a clear increase, whereas PAs with smaller excess charges are unaffected. A further decrease in temperature to $T \approx 1$ also lets the PAs with $Q_{\text{tot}}=24$ and 32 expand significantly. At $T \approx 0.1$ we find $R_g > R_{g,0}$ for all chains with Q_{tot} between 16 and 64; note that the highly charged PAs with $Q_{\text{tot}}=56$ and 64 are almost completely stretched, $R_g^2 = b^2 N^2 / 12 \approx 341$, so that their finite extensibility comes into play. On the other hand, at $T \approx 0.1$ the chains with $Q_{\text{tot}}=0$ and $Q_{\text{tot}}=4$ are in a collapsed state with $R_g < R_{g,0}$. The boundary between the two cases is given by PAs with $Q_{\text{tot}}=8$, for which $R_g \approx R_{g,0}$, i.e., the change in the radius of gyration is small.

We note first that these results reproduce the numerical observations of Kantor and Kardar [16] which they found using the bond-fluctuation method. Furthermore the results support the argument given above: By lowering the temperature PAs with Q_{tot} above a critical value (here around 8) expand, whereas chains with Q_{tot} below this value collapse. Furthermore using Eq. (6) as an estimate for the temperature below which the electrostatic interactions are relevant we have $T_{Q_{\text{tot}}} \approx (Q_{\text{tot}}^2 - q^2 N) / R_g \approx (Q_{\text{tot}}^2 - 64) / 30$. This leads to $T_{64} \approx 134$, $T_{32} \approx 32$, $T_{16} \approx 6$, $T_8 \approx 0$, and $T_0 \approx 2$, in good agreement with the numerical findings.

Up to now we have focused only on R_g , which is a measure for the overall size of the chains. Now, an interesting

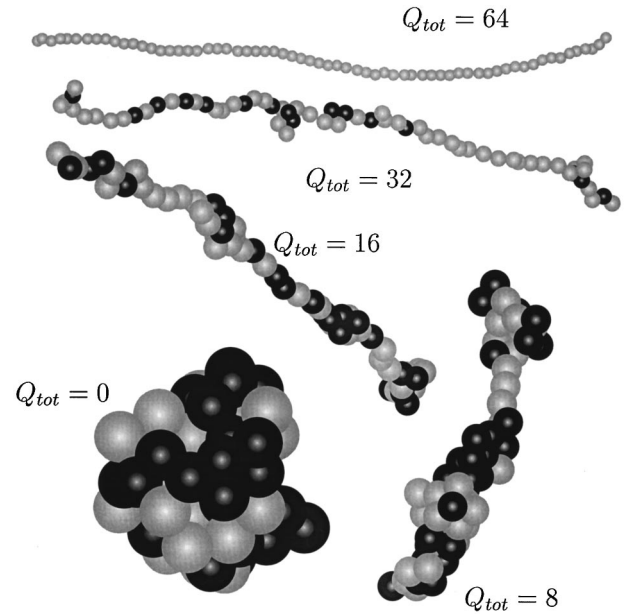


FIG. 2. Snapshots of conformations of PAs with different excess charges Q_{tot} ($q=1$) at the temperature $T=0.1$. The diameter of the spheres corresponds to the excluded volume range, the shades indicate their (opposite) charges.

question concerns the typical shape of the PA. An important ingredient here is the surface tension; in analogy to charged drops and taking the PAs' connectivity into account, Kantor and Kardar [16] suggest that PAs may stretch out in a necklace shape. Now, inhomogeneities in the charge distribution along the chain may lead to a disordered necklace. To stress this we display in Fig. 2 some PAs' conformations at $T=0.1$. The polyelectrolyte with $Q_{\text{tot}}=64$ is almost completely stretched; the same holds for the PA with $Q_{\text{tot}}=32$. On the other hand, the chains with $Q_{\text{tot}}=16$ and 8 show clearly stretched and condensed parts, i.e., they constitute random necklaces. Finally, the PA with vanishing total charge is collapsed and forms a spherical globule. We find it worth stressing that the PA with $Q_{\text{tot}}=8$ has indeed $R_g \approx R_{g,0}$, but that its shape differs strongly from that of an uncharged chain; the PA is a random necklace.

III. CONFORMATIONAL PROPERTIES OF WEAKLY CHARGED PAS IN EXTERNAL FIELDS

This section is devoted to the behavior of weakly charged PAs exposed to external electrical fields; the case of strongly charged PAs is discussed in the next section. We are thus in the WCL domain, i.e., where Eq. (4) is fulfilled. Furthermore, since we analyzed the WCL case for $Q_{\text{tot}} \neq 0$ extensively in Refs. [24,26,28], we focus here mainly on the $Q_{\text{tot}}=0$ case.

In order to calculate the conformational properties of PAs in external fields we use an extension of an approach pioneered by Pincus [46] (cf. also Ref. [47]): Pincus considered a polymer under traction so that two forces, \vec{F} and $-\vec{F}$, act on its ends. A realization is, e.g., a chain with two oppositely charged monomers at its ends ($q_0 = -q$, $q_{N-1} = +q$ and $q_k = 0$ otherwise) in an external electrical field \vec{E} , so that $\vec{F} = q\vec{E}$ [47]. The elongation ΔL of the chain may be written as

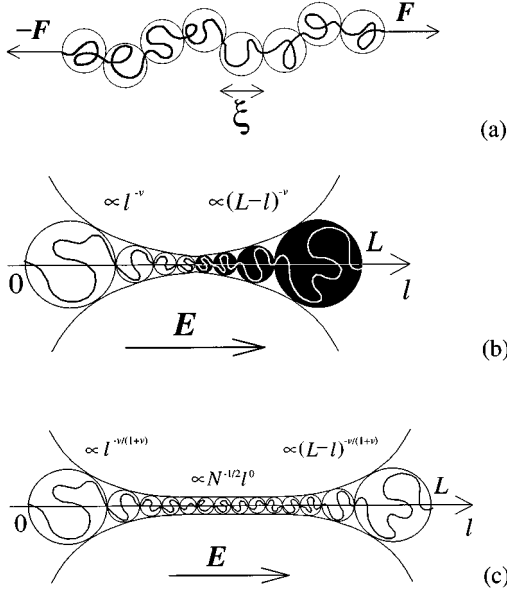


FIG. 3. (a) A polymer under traction (external force F). The chain breaks up into a string of Pincus blobs of size $\xi = T/F$. (b) A diblock PA in an external electrical field (tug of war). The chain consists of a string of Pincus blobs of different sizes, constituting a double trumpet. (c) Equilibrium conformation of a random PA [using \bar{Q}_n , Eq. (16), as charge distribution; see text for details].

$$\Delta L = R \varphi \left(\frac{R}{\xi} \right), \quad (7)$$

where φ is a dimensionless function, R denotes the size of the unperturbed coil, $R = bN^\nu$, and ξ is the characteristic length of the problem, $\xi = T/F$ with $F = |\vec{F}|$. For small F , such that $\xi \gg R$, the response is linear, i.e., $\varphi(x) \propto x$; this leads to

$$\Delta L \approx \frac{b^2 N^{2\nu} F}{T}. \quad (8)$$

On the other hand, for $\xi \ll R$ the chain breaks up into a one-dimensional string of blobs of size ξ [cf. Fig. 3(a)]. Then the elongation, Eq. (7), is proportional to N , which leads to the requirement that $\varphi(x)$ obeys a power law, namely, $\varphi(x) \propto x^\alpha$ with $\alpha = (1 - \nu)/\nu$. Hence for large F

$$\Delta L \approx Nb \left(\frac{bF}{T} \right)^{(1-\nu)/\nu} = \begin{cases} Nb \frac{bF}{T} & \text{in a } \theta \text{ solvent} \\ Nb \left(\frac{bF}{T} \right)^{2/3} & \text{in a good solvent.} \end{cases} \quad (9)$$

Note that in a good solvent the deformation is nonlinear in the applied force, $\Delta L \propto F^{2/3}$. Computer results support the scaling argument; thus using the bond-fluctuation method the two regimes of Eqs. (8) and (9) were observed clearly [48].

We focus now on the PA's shape in the WCL, for prescribed charge distributions $\{q_k\}$. The problem was considered analytically by Schiessel and Blumen [26,28], and we

recall here the main ideas. We introduce the cumulative charge variable Q_k defined by

$$Q_k = \sum_{i=1}^k q_i \quad \text{for } 1 \leq k \leq N. \quad (10)$$

Since we focus on PAs with $Q_{\text{tot}} = 0$ we also have $Q_N = Q_{\text{tot}} = 0$. Pick out an arbitrary segment, say the n th one. Then the segment divides the chain into two halves, one carrying the cumulative charge Q_n and—due to $Q_{\text{tot}} = 0$ —the other one the charge $-Q_n$. In an external electrical field E the force acting on segment n is given by $F_n = Q_n E$. Thus we encounter here a situation in which the tension F_n is segment dependent and where the stretching of the chain is not uniform. In Refs. [26, 28] we have generalized Eqs. (8) and (9) to this situation, following Brochard-Wyart [49], who considered the nonuniform deformation of tethered chains in solvent flows. Let $\xi_n = T/F_n$ be the n -dependent size of the Pincus blobs and l_n the position of the n th monomer in the direction of the field. In the case of a small force at n , i.e., for $\xi_n \gg R$, the local elongation at site n is, following Eq. (8),

$$dl_n \approx \frac{b^2 F_n}{T} n^{2\nu-1} dn, \quad (11)$$

whereas in the strong tension regime one finds from Eq. (9)

$$dl_n \approx b \left(\frac{bF_n}{T} \right)^{(1-\nu)/\nu} dn. \quad (12)$$

Let us illustrate this nonuniform stretching in the case of a symmetric diblock PA with $q_k = -q$ for $1 \leq k \leq N/2$ and $q_k = q$ for $N/2 < k \leq N$. Its cumulative charge distribution is given by

$$Q_k = \begin{cases} kq & \text{for } k \leq N/2 \\ (N-k)q & \text{for } k > N/2. \end{cases} \quad (13)$$

Integrating Eq. (11) over n one finds at small fields, i.e., as long as $E < T/(qbN^{1+\nu})$ holds, that the deformation obeys

$$\Delta L \approx \frac{b^2 q E}{T} N^{2\nu+1}. \quad (14)$$

Note that Eq. (14) also follows when one replaces in Eq. (8) F by an effective force $F_{\text{eff}} = qEN$. In the case of strong fields Eq. (13) leads to

$$\Delta L \approx b \left(\frac{bqE}{T} \right)^{(1-\nu)/\nu} N^{1/\nu}. \quad (15)$$

Again, Eq. (15) can be obtained by simply replacing F in Eq. (9) by $F_{\text{eff}} = qEN$. This means that Eq. (7) is still applicable when one sets $\xi = \xi_{\text{eff}} = T/F_{\text{eff}}$.

Let us now compare the outcome of this scaling argument with the results of MD simulations. Based on the fact that we are in the WCL case we switched off the electrostatic interaction between the charges, i.e., we set from the start $U_{ij}^C \equiv 0$, a fact which improves the performance of the algorithm. We have considered diblock PAs at $T = 0.1$ and varied both their length N and the field strength E . The results are dis-

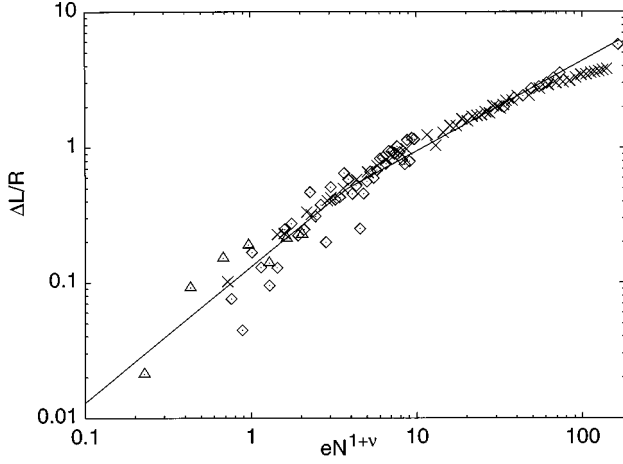


FIG. 4. Field-induced stretching of diblock PAs. Depicted is the relative stretching of the chain $\Delta L/R$ as a function of $eN^{\nu+1}$; e denotes the dimensionless field strength $e = bqE/T$. The straight lines correspond to the linear and to the Pincus regime (see text for details).

played in Fig. 4, where the crosses indicate PAs with $N = 100$ for various E (ranging from $E = 5 \times 10^{-5}$ to $E = 0.077$), the diamonds indicate PAs under $E = 0.002$, whose lengths range from $N = 10$ to 300 and the triangles PAs under $E = 0.0002$, with length varying from $N = 20$ to 90. Following Eq. (7) we plotted in Fig. 4 $\Delta L/R$ as a function of R/ξ_{eff} . As can be readily seen, the data for different N and E collapse into a master curve. Furthermore, the two regimes $\Delta L \propto E$ for $R/\xi_{\text{eff}} < 3$ and $\Delta L \propto E^{2/3}$ for $R/\xi_{\text{eff}} > 3$ are clearly visible; in Fig. 4 we also indicated the expected slopes, 1 and $\frac{2}{3}$. We note that for very large values of E (say for $R/\xi_{\text{eff}} > 20$ for the $N = 100$ PA) the numerical results deviate from what is expected based on scaling arguments: The latter are invalid for very large fields, due to the finite extensibility of the PA chains (see below).

From the scaling picture given above one can also infer the global shape of the PA [28]. The sizes ξ_n of the Pincus blobs obey $\xi_n \propto F_n^{-1} \propto n^{-1}$ for $n < N/2$ and $\xi_n \propto (N-n)^{-1}$ for $n > N/2$, see Eq. (13). Hence the blob sizes increase towards the ends of the PA, as shown in Fig. 3(b), and the PA is symmetric with respect to its center. Making use of $l_n \propto n^{1/\nu}$ one finds for $n < N/2$ that the blob sizes go as $\xi_{n(l)} \propto n(l)^{-1} \propto l^{-\nu}$; this behavior is also indicated in Fig. 3(b). The PA's shape can be compared to that of a tethered chain subjected to a uniform solvent flow [49]: Here the force increases from the free end to the grafted one, and the blob sizes decrease in the same direction; this results in a trumpetlike shape. Our PAs, which are exposed to a kind of tug of war, show a similar shape, having, however, two trumpetlike ends.

At sufficiently high field strengths the double-trumpet picture breaks down, namely, when the size of the central Pincus blob $\xi_{N/2}$ gets to be of the order of the persistence length b , i.e., at a field strength E of around $T/(qbN)$. At still higher field strengths the middle part of the PA is completely stretched, while its ends still show Pincus-type behavior. A similar finding was reported by Brochard-Wyart for polymer chains under strong flows, and the corresponding regime was called ‘‘stem and flower’’ [50]. Here, in the tug of war situation, for sufficiently large E the PA's shape consists of two

flowers connected by a stem. The value of E at which this behavior sets in is clearly visible in Fig. 4 at large R/ξ_{eff} , where, due to the chain's finite extensibility the numerically determined values cease to obey scaling.

In Fig. 5 we display several conformations of diblock PAs with $N = 100$; shown are (a) the linear regime, (b) the Pincus regime (double-trumpet), and (c) the stem and flower regime. We show together both a particular realization, as well as the probability density (given by different shades of gray) of the PAs positions projected on the YZ plane. The density is calculated by averaging over 200 conformations, and making use of the symmetry with respect to the center of mass, the latter being fixed at the origin. From the density plots the three distinct patterns of diblock PAs are evident; we find (a) a slightly elongated coil, (b) the double-trumpet, and (c) the stem-and-flower conformation. Our findings can be directly compared to experimental visualizations of trumpetlike structures, i.e., as determined by fluorescence microscopy of DNA segments, which are dragged at one end by optical or magnetic tweezers [51,52]. Thus in Ref. [52] the three shapes (a slightly perturbed coil, a single trumpet, a stem with one flower) are clearly visible.

We end this section by sketching the situation encountered for random charge distributions $\{q_n\}$. In this case an appropriate approximation is to calculate the typical deformation of such chains from the quenched average of the cumulative charge variable, \bar{Q}_n (see Ref. [26] for details; this procedure should not be confused with a preaveraging over randomness, say, in the partition function, which leads to an effectively annealed system). For neutral PAs, i.e., for $Q_{\text{tot}} = 0$, the charge correlations are given by Eq. (5). Averaged over different distributions $\{q_n\}$ leads to the cumulative charge variable \bar{Q}_n :

$$\bar{Q}_n = \sqrt{\langle Q_n^2 \rangle} = q \sqrt{fn(1-n/N)}. \quad (16)$$

In this picture the sizes of the Pincus blobs obey

$$\xi_n = \frac{T}{\sqrt{fn(1-n/N)qE}}, \quad (17)$$

i.e., one again finds a double trumpet, as displayed in Fig. 3(c). The end-to-end distance is

$$\Delta L \approx bN \left(\frac{\sqrt{fn}qEb}{T} \right)^{(1-\nu)/\nu} = \begin{cases} bN \frac{\sqrt{fn}qEb}{T} & \text{for } \nu = \frac{1}{2} \\ bN \left(\frac{\sqrt{fn}qEb}{T} \right)^{2/3} & \text{for } \nu = \frac{3}{5}. \end{cases} \quad (18)$$

Note that the case $\nu = \frac{1}{2}$ is in accordance with the result of an exact calculation [cf. Eq. (31) of Ref. [28]].

Equation (18) can be inferred from Eq. (9) by simply replacing F by an effective force F_{eff} of the order of $q\sqrt{fNE}$; this effective force can be envisaged to arise from the usual charge fluctuations, which go as $q\sqrt{fN}$. Of course, this picture (the *monoblock approximation* of Ref. [53]) is

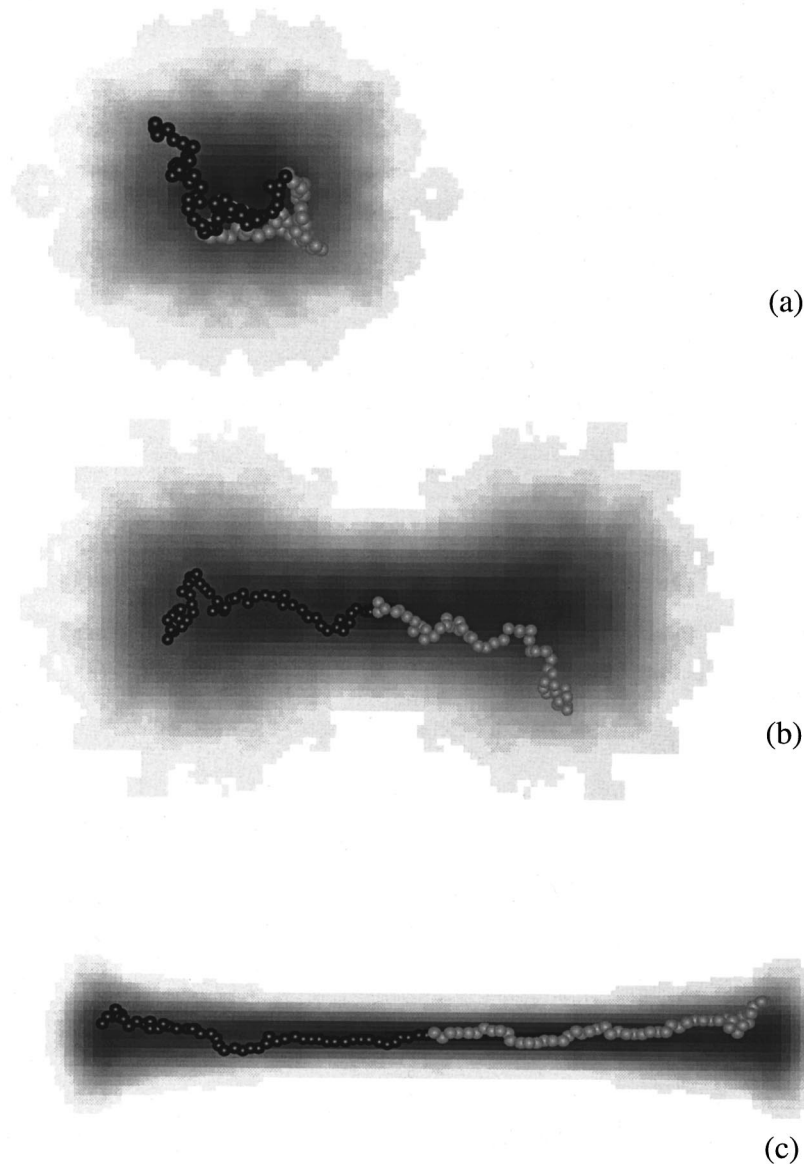


FIG. 5. Density plots of PAs at $T=0.1$ in the (a) linear regime (slightly perturbed coil) with $E=0.0005$, (b) Pincus regime (double trumpet) with $E=0.005$, and (c) stem-and-flower regime with $E=0.02$. In each case we also present a snapshot of a particular realization.

very simplified, since it implies a string of equally sized Pincus blobs, each of dimension $\xi_{\text{eff}}=T/F_{\text{eff}}$.

IV. CONFORMATIONAL PROPERTIES OF STRONGLY CHARGED PAS IN EXTERNAL FIELDS

In this section we investigate the behavior of PAs in external fields, when the intramolecular charge interactions are strong. As already stressed in Sec. II, PAs with $Q_{\text{tot}}=0$ collapse into a globule, whose volume is given by Eq. (2). On the other hand the PA's *shape* is determined by the surface tension and—when present—by the external fields. In this picture the free energy of the surface has the form

$$F_S = \gamma S, \quad (19)$$

where S denotes the PA's surface and γ the surface tension between globule and solvent. Now, by considering the Debye blobs at the globule's surface one has $\gamma \approx T/r_D^2$ [15]. In

the absence of external perturbations the PA minimizes its energy by minimizing its surface, i.e., by assuming a spherical shape.

Schiessel and Blumen [26] and Dobrynin, Rubinstein, and Joanny [32] have investigated the response of such PA droplets to external electrical fields. Reference [26] argues that in moderate electrical fields the PAs assume dumbbell-like shapes (this is similar to the behavior of charged liquid drops [54]). The surface-dominated scenario stops at a critical field strength E_{c1} , where the surface tension cannot counterbalance the external force anymore; above E_{c1} the PA extends, and shows strongly stretched regions formed by Pincus blobs, separated by condensates of Debye blobs [26]. On the other hand, the authors of Ref. [32] follow a different approach and analyze the conditions under which strings and globules may coexist; from this they determine the critical field strength E_{c2} , which separates globular from stretched states. Interestingly, Refs. [26] and [32] report different val-

ues for the critical field strength, having, namely, $E_{c2} \ll E_{c1}$.

In this section we sketch both approaches and show that the differences between them are related to the metastability of the collapsed state. Furthermore, we present molecular-dynamics simulations which display hysteresis, and hence imply metastable states.

Let us start with a simplified version of the argument given by Schiessel and Blumen [26]. In an electrical field the surface tension has to balance the electrostatic energy of the electric dipole induced by the external field. In Sec. III we have shown that a random PA in a strong external field can be viewed as being a dipole whose charges $\pm q\sqrt{fN}$ are a distance ΔL apart. Making use of this picture for a PA with a nearly globular shape [26,32] leads to its free energy:

$$F = F_S + F_{\text{ext}} \approx \gamma S - q\sqrt{fNE}\Delta L. \quad (20)$$

Under weak external fields the PA extends into a prolate ellipsoid, with its axis parallel to the field. We denote by $L(E) = R + \Delta L$ the PA's length in field direction, with R being the radius of the unperturbed spherical globule. For small E , so that $\Delta L \ll R$, the growth ΔS in the PA's surface area is quadratic in ΔL , since then the PA's shape differs only slightly from a sphere (minimal surface). Thus ΔS scales as $\Delta S \approx (\Delta L)^2$. Minimizing Eq. (20) with respect to ΔL leads to

$$\Delta L \approx \frac{q\sqrt{fNE}}{\gamma}, \quad (21)$$

i.e., ΔL is linear in E . A more rigorous approach leads to the same result, cf. Eq. (19) of Ref. [26].

With increasing E the globule becomes more and more elongated. Reference [26] argues that then the PA becomes dumbbell-like and calculates the critical field E_{c1} . We can reproduce this result by assuming the PA to be a cylinder of height $L(E)$ and diameter $D(E)$. This cylinder has to fulfill the fixed volume condition, Eq. (2), which takes here the form $L(E)D(E)^2 \approx V$.

We calculate now the critical field strength E_{c1} at which the surface tension cannot counterbalance the external force anymore. E_{c1} can be found by considering the change in free energy $dF = dF_S + dF_{\text{ext}}$ which accompanies a small virtual deformation of the cylinder, namely, its lengthening from L to $L + dL$. Then the change in F is the sum of a positive term (due to the increase in surface area) and of a negative term (due to the increase of the dipole moment); specifically we have

$$dF \approx \gamma D(E)dL - q\sqrt{fNE}dL. \quad (22)$$

Thus the cylinder becomes unstable at $E = E_{c1} \approx \gamma D(E_{c1}) / (q\sqrt{fN})$. A more elaborated analysis [26] shows furthermore that at $E = E_{c1}$ the radius a of the dumbbell's neck fulfills $a \approx 0.5R$, which translates here into $D(E_{c1}) \approx R$. Thus we find that E_{c1} obeys

$$E_{c1} \approx \frac{\gamma R}{q\sqrt{fN}}, \quad (23)$$

which has indeed the same form as Eq. (22) of Ref. [26].

At $E \approx E_{c1}$ the surface tension cannot stabilize the elongated globule anymore, which then breaks up into a string of droplets connected by strongly stretched portions [26,28]. Let us first imagine that the interactions between the charges are switched off; these interactions can be incorporated *a posteriori*, as we proceed to show. Without such interactions one has [using \bar{Q}_n , Eq. (16), as charge distribution] the situation depicted in Fig. 3(c); the sizes of the Pincus blobs are given by Eq. (17), and the total elongation obeys Eq. (18). The picture can be further simplified by using the monoblock approximation, with monodisperse Pincus blobs of size $\xi_{\text{eff}} \approx T/F_{\text{eff}}$, with $F_{\text{eff}} \approx q\sqrt{fNE}$ (see the discussion at the end of Sec. III).

Let us now consider the role of the interaction between the charges. Already after the breakup at $E \approx E_{c1}$ the electrostatic energy of the majority of Pincus blobs is much smaller than the thermal energy: One has (in the monoblock approximation) $\xi_{\text{eff}}/r_D \approx r_D/R \ll 1$, so that the electrostatic interaction leads only to a small perturbation. In general one has to pay attention to the situation near the PA's ends, where the Pincus blobs are largest, being still condensates of Debye blobs. To be more specific: consider the chain's half containing the monomer $n=0$. Here any monomer n belongs to a condensate as long as $\xi_n > r_D$. Setting $\xi_{n1} = r_D$ and $E = E_{c1}$ one finds from Eqs. (17) and (23) $n_1 \approx (r_D/R)^2 N \ll N$. Thus using \bar{Q}_n , Eq. (16), as charge distribution, only a small amount of material is still in the condensed state, i.e., for $E > E_{c1}$ Eq. (18) is still a good approximation for the total extension.

As discussed in Refs. [26] and [28] using \bar{Q}_n , Eq. (16), as charge distribution allows calculation of the "typical" conformation of PAs. Note, however, that for a given quenched distribution $\{q_n\}$ the shape of an individual PA may deviate from this picture. Thus there may occur zig-zag configurations with condensates at the turning points. Neglecting these details by using \bar{Q}_n , or even applying—as a further simplification—the monoblock approximation is often helpful, since these two approaches can be easily handled and lead—as can be shown rigorously in the Θ case [28]—to correct scaling relations.

Dobrynin, Rubinstein, and Joanny [32] evaluated in the monoblock picture the critical field strength E_{c2} at which a transition takes place between the globular and the extended state. They considered the chemical potentials μ_{glob} of the globular and $\mu_{\text{str}}(E)$ of the stretched states. The field strength E_{c2} follows then from $\mu_{\text{str}}(E_{c2}) = \mu_{\text{glob}}$. Using Eqs. (1) and (2) one finds for $\mu_{\text{glob}} = \partial F_e / \partial N$:

$$\frac{\mu_{\text{glob}}}{T} \approx - \left(\frac{fl_B}{b} \right)^{1/(1-\nu)}. \quad (24)$$

On the other hand $\mu_{\text{str}}(E)$ follows from the free energy $F_{\text{str}}(E)$ of the stretched state, $F_{\text{str}}(E) = -q\sqrt{fNE}\Delta L$, with ΔL given by Eq. (18). Thus one has

$$\frac{\mu_{\text{str}}(E)}{T} \approx - \left(\frac{bq\sqrt{fNE}}{T} \right)^{1/\nu}. \quad (25)$$

Equating the chemical potentials, Eqs. (24) and (25), leads to

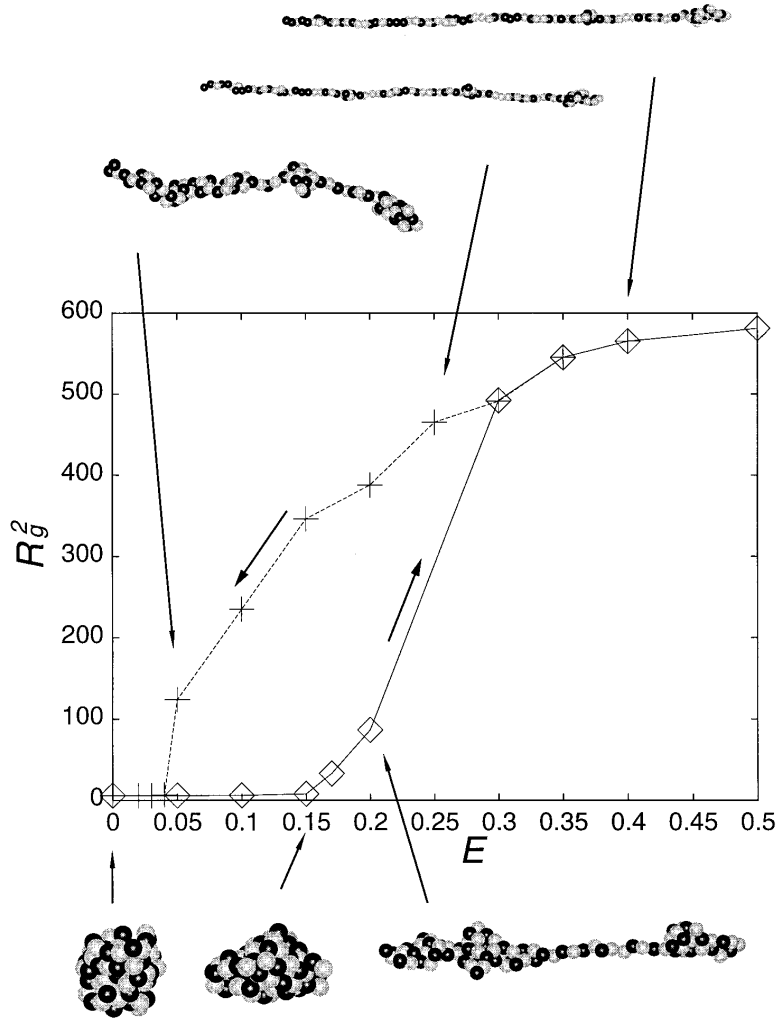


FIG. 6. PA chain in an external electrical field. Depicted is R_g^2 ($b=1$) as a function of E together with some typical configurations ($N=100$, $T=0.02$). Note the hysteresis effect (see text for details).

$$E_{c2} \approx \frac{T}{bq\sqrt{fN}} \left(\frac{fl_B}{b} \right)^{\nu(1-\nu)}. \quad (26)$$

The critical field strength E_{c2} can also be obtained by comparing the typical size of the Pincus blobs $\xi_{\text{eff}}(E) \approx T/(q\sqrt{fNE})$ with the Debye length $r_D = (V/fNl_B)^{1/2} = b(b/fl_B)^{\nu(1-\nu)}$ [32]. The Pincus blobs are unstable as long as $\xi(E) > r_D$, so that the transition from collapsed to stretched states occurs at $\xi(E_{c2}) = r_D$, which again leads to Eq. (26).

Let us now compare the critical field strengths E_{c1} and E_{c2} . From Eqs. (23) and (26) one has

$$\frac{E_{c1}}{E_{c2}} \approx \frac{\gamma Rb}{T} \left(\frac{b}{fl_B} \right)^{\nu(1-\nu)} \approx \left(\frac{fN^{1-\nu}l_B}{b} \right)^{1/(3-3\nu)}. \quad (27)$$

In the Debye-Hückel regime, under the condition of Eq. (3) one has $E_{c1}/E_{c2} \gg 1$, i.e., the critical field strength E_{c1} (which is based on the surface tension) is much larger than E_{c2} (which follows from the comparison of the free energies of the globular and of the stretched states).

This difference can be understood as being due to the metastability of the globular state. In the regime of interme-

mediate field strengths, $E_{c2} < E < E_{c1}$, the analysis of Dobrynin, Rubinstein, and Joanny [32] shows that the free energy of the stretched state is lower than the free energy of the globule. On the other hand, the argument of Schiessel and Blumen [26] demonstrates the crucial role of the surface tension: Starting from the globular state one needs a field strength E_{c1} which is much higher than E_{c2} in order to reach the global minimum (stretched state).

As already mentioned in Ref. [26], the surface-controlled scenario can be circumvented when one starts with a highly extended state at $E > E_{c1}$ and then decreases E moderately. In this case the transition from the stretched to the globular state sets in when the typical size of the Pincus blobs reaches the Debye length, i.e., at $E = E_{c2}$. Clearly, for a given realization $\{q_n\}$ of the charge distribution one has an inhomogeneous tension along the chain; thus for different parts of the chain the transition takes place at different field strengths. This may lead to a broadening of the transition region around E_{c2} .

The metastability of the globule is due to the nonlocal coupling of the total external force to the PA. If the force $F_{\text{eff}} = q\sqrt{fNE}$ would act only on a single monomer (or on a small part of the chain) a field strength of E_{c2} would suffice

in order to unravel the globule (such a situation was considered in Ref. [55]). This situation (which is assumed implicitly in the monoblock approximation) leads to a critical field strength of E_{c2} . At $b = fN^{\nu-1}l_B$ which marks the border to the WCL [cf. Eq. (4)] the electrostatic energy of the PA is of the order of the thermal energy, i.e., here one has no condensation effects and thus no surface tension (indeed one finds here $r_D = R = bN^\nu$). Consequently one has $E_{c1} = E_{c2}$, cf. Eq. (27), i.e., here the hysteresis effect vanishes.

We close this section by reporting that MD simulations indeed show hysteresis. In Fig. 6 we present simulation results obtained for a PA of length $N = 100$ with vanishing total charge ($Q_{\text{tot}} = 0$); the chain consists of 50 positively and 50 negatively charged monomers, which are distributed in random fashion. We start with the globular state at $T = 0.02$ and $E = 0$. Then by increasing the field strength in a quasistatic manner up to $E = 0.15$ (diamonds in Fig. 6) we observe the deformation of the chain into an elongated globule; during this process R_g^2 increases only slightly. At $E \approx 0.15$ a faster increase of R_g^2 sets in, which is accompanied by the breakup of the globule into a random necklace structure (cf. the example configuration at $E = 0.2$). Around $E = 0.3$ a strongly stretched state is reached, where only a small amount of monomers still form condensates. After having reached the field strength $E = 0.5$ and a very extended PA, we decrease E in a quasistatic manner. In the regime of stretched states up to $E \geq 0.3$ the values of R_g^2 for increasing E (diamonds) and for decreasing E (crosses) are practically identical. However, by further decreasing the field strength we observe hysteresis: the R_g values are history dependent and are much larger for decreasing than for increasing E . On the decreasing E branch the chain consists of stretched and collapsed portions (even for the relatively low value of $E = 0.05$, cf. the corresponding snapshot) whereas on the increasing E branch the chain is globular, being almost unperturbed by the external force. On the decreasing E branch the PA returns to globular

shape only near $E = 0.04$. In summary our simulations display clearly hysteresis; we hasten, however, to note that a quantitative comparison with the theoretical predictions (especially where the droplet picture is concerned) requires the use of larger chains in the simulations.

V. CONCLUSION

In conclusion, we have studied the behavior of single PAs by means of MD simulations and of scaling arguments. PAs with vanishing total charge form spherical globules, whereas chains with strong excess charges display stretched configurations; the total charge $Q_{\text{tot}} \approx q\sqrt{fN}$ marks the borderline between these two regimes. Our MD simulations confirm this picture. Furthermore, we investigated the influence of an external field on the conformations of PAs. In the case of negligible coupling between the charges (weak-coupling limit) the chains show three typical regimes: (a) a regime of linear response to small fields (slightly perturbed coil), (b) the Pincus regime at intermediate field strengths (a double-trumpet conformation), and (c) the stem-and-flower regime at strong fields (due to the finite extensibility of the PA). On the other hand, in the case of strong coupling between its charges a PA globule is unstable in an electrical field. For increasing E fields the PA's shape is controlled by the surface tension, whereas under decreasing E fields the interplay between condensed and stretched parts dominates the behavior; a particularly remarkable consequence of this scenario is the occurrence of hysteresis.

ACKNOWLEDGMENTS

The authors are indebted to Dr. J.-U. Sommer for fruitful discussions. The support of the DFG (through SFB 428, Graduiertenkolleg) and the Fonds der Chemischen Industrie is gratefully acknowledged.

-
- [1] S. F. Edwards, P. R. King, and P. Pincus, *Ferroelectrics* **30**, 3 (1980).
 - [2] C. Qian and A. L. Kholodenko, *J. Chem. Phys.* **89**, 5273 (1988).
 - [3] Y. Kantor and M. Kardar, *Europhys. Lett.* **14**, 421 (1991).
 - [4] P. G. Higgs and J. F. Joanny, *J. Chem. Phys.* **94**, 1543 (1991).
 - [5] Y. Kantor, H. Li, and M. Kardar, *Phys. Rev. Lett.* **69**, 61 (1992).
 - [6] M. Schulz and S. Stepanow, *J. Chem. Phys.* **98**, 5074 (1993).
 - [7] J.-M. Corpart and F. Candau, *Macromolecules* **26**, 1333 (1993).
 - [8] J. M. Victor and J. B. Imbert, *Europhys. Lett.* **24**, 189 (1993).
 - [9] Y. Kantor, M. Kardar, and H. Li, *Phys. Rev. E* **49**, 1383 (1994).
 - [10] J. Wittmer, A. Johner, and J. F. Joanny, *Europhys. Lett.* **24**, 263 (1993).
 - [11] M. Skouri, J. P. Munch, S. J. Candau, S. Neyret, and F. Candau, *Macromolecules* **27**, 69 (1994).
 - [12] A. M. Gutin and E. I. Shakhnovich, *Phys. Rev. E* **50**, R3322 (1994).
 - [13] J.-F. Joanny, *J. Phys. II* **4**, 1281 (1994).
 - [14] Y. Kantor and M. Kardar, *Europhys. Lett.* **27**, 643 (1994).
 - [15] A. V. Dobrynin and M. Rubinstein, *J. Phys. II* **5**, 677 (1995).
 - [16] Y. Kantor and M. Kardar, *Phys. Rev. E* **51**, 1299 (1995).
 - [17] Y. Kantor and M. Kardar, *Phys. Rev. E* **52**, 835 (1995).
 - [18] H. Schiessel, G. Oshanin, and A. Blumen, *J. Chem. Phys.* **103**, 5070 (1995).
 - [19] Y. Levin and M. C. Barbosa, *Europhys. Lett.* **31**, 513 (1995).
 - [20] H. Schiessel, G. Oshanin, and A. Blumen, *Macromol. Theory Simul.* **5**, 45 (1996).
 - [21] D. Bratko and A. K. Chakraborty, *J. Phys. Chem.* **100**, 1164 (1996).
 - [22] D. Ertaş and Y. Kantor, *Phys. Rev. E* **53**, 846 (1996).
 - [23] D. Srivastava and M. Muthukumar, *Macromolecules* **29**, 2324 (1996).
 - [24] H. Schiessel and A. Blumen, *J. Chem. Phys.* **104**, 6036 (1996).
 - [25] M. C. Barbosa and Y. Levin, *Physica A* **231**, 467 (1996).
 - [26] H. Schiessel and A. Blumen, *J. Chem. Phys.* **105**, 4250 (1996).
 - [27] A. Diehl, M. C. Barbosa, and Y. Levin, *Phys. Rev. E* **54**, 6516 (1996).

- [28] H. Schiessel and A. Blumen, *Macromol. Theory Simul.* **6**, 103 (1997).
- [29] R. G. Winkler and P. Reineker, *J. Chem. Phys.* **106**, 2841 (1997).
- [30] R. Everaers, A. Johner, and J.-F. Joanny, *Europhys. Lett.* **37**, 275 (1997).
- [31] B.-Y. Ha and D. Thirumalai, *J. Phys. II* **7**, 887 (1997).
- [32] A. V. Dobrynin, M. Rubinstein, and J.-F. Joanny, *Macromolecules* **30**, 4332 (1997).
- [33] D. Loomans, H. Schiessel, and A. Blumen, *J. Chem. Phys.* **107**, 2636 (1997).
- [34] H. Schiessel, I. M. Sokolov, and A. Blumen, *Phys. Rev. E* **56**, R2390 (1997).
- [35] H. Schiessel (unpublished).
- [36] T. E. Creighton, *Proteins: Their Structure and Molecular Properties* (Freeman, San Francisco, 1984).
- [37] K. A. Dill *et al.*, *Protein Sci.* **4**, 561 (1995).
- [38] E. Shakhnovich, V. Abkevich, and O. Ptitsyn, *Nature (London)* **96**, 379 (1996).
- [39] V. S. Pande, A. Yu. Grosberg, C. Joerg, M. Kardar, and T. Tanaka, *Phys. Rev. Lett.* **77**, 3565 (1996).
- [40] M. Mezard, G. Parisi, and M. A. Virasoro, *Spin Glass Theory and Beyond* (World Scientific, Singapore, 1987).
- [41] K. Binder and A. P. Young, *Rev. Mod. Phys.* **58**, 801 (1986).
- [42] L. D. Landau and E. M. Lifschitz, *Statistical Physics* (Pergamon, New York, 1981).
- [43] I. Carmesin and K. Kremer, *Macromolecules* **21**, 2819 (1988).
- [44] H.-P. Deutsch and K. Binder, *J. Chem. Phys.* **94**, 2294 (1991).
- [45] G. Grest and K. Kremer, *Phys. Rev. A* **33**, 3628 (1986).
- [46] P. Pincus, *Macromolecules* **9**, 368 (1976).
- [47] P. G. de Gennes, *Scaling Concepts in Polymer Physics* (Cornell University Press, Ithaca, 1979).
- [48] M. Wittkop, J.-U. Sommer, S. Kreitmeier, and D. Göritz, *Phys. Rev. E* **49**, 5472 (1994).
- [49] F. Brochard-Wyart, *Europhys. Lett.* **23**, 105 (1993).
- [50] F. Brochard-Wyart, *Europhys. Lett.* **30**, 387 (1995).
- [51] T. T. Perkins, D. E. Smith, R. G. Larson, and S. Chu, *Science* **268**, 83 (1995).
- [52] D. Wirtz, *Phys. Rev. Lett.* **75**, 2436 (1995).
- [53] F. Brochard-Wyart, H. Hervet, and P. Pincus, *Europhys. Lett.* **26**, 511 (1994).
- [54] J. D. Sherwood, *J. Fluid Mech.* **188**, 133 (1988).
- [55] A. Halperin and E. B. Zhulina, *Europhys. Lett.* **15**, 417 (1991).